Molecular Cancer Therapeutics

$\alpha_V\beta_3$ Integrin-Targeted Radionuclide Therapy with ^{64}Cu-cyclam-RAFT-c(-RGDfK-)$_4$

Zhao-Hui Jin[1], Takako Furukawa[1], Mélissa Degardin[2], Aya Sugyo[1], Atsushi B. Tsuji[1], Tomoteru Yamasaki[1], Kazunori Kawamura[1], Yasuhisa Fujibayashi[1], Ming-Rong Zhang[1], Didier Boturyn[2], Pascal Dumy[3], and Tsuneo Saga[1]

Abstract

The transmembrane cell adhesion receptor $\alpha_V\beta_3$ integrin ($\alpha_V\beta_3$) has been identified as an important molecular target for cancer imaging and therapy. We have developed a tetrameric cyclic RGD (Arg-Gly-Asp) peptide–based radiotracer ^{64}Cu-cyclam-RAFT-c(-RGDfK-)$_4$, which successfully captured $\alpha_V\beta_3$-positive tumors and angiogenesis by PET. Here, we subsequently evaluated its therapeutic potential and side effects using an established $\alpha_V\beta_3$-positive tumor mouse model. Mice with subcutaneous U87MG glioblastoma xenografts received single administrations of 37 and 74 MBq of ^{64}Cu-cyclam-RAFT-c(-RGDfK-)$_4$ (37 MBq/nmol), peptide control, or vehicle solution and underwent tumor growth evaluation. Side effects were assessed in tumor-bearing and tumor-free mice in terms of body weight, routine hematology, and hepatorenal functions. Biodistribution of ^{64}Cu-cyclam-RAFT-c(-RGDfK-)$_4$ with ascending peptide doses (0.25–10 nmol) and with the therapeutic dose of 2 nmol were determined at 3 hours and at various time points (2 minutes–24 hours) postinjection, respectively, based on which radiation-absorbed doses were estimated. The results revealed that ^{64}Cu-cyclam-RAFT-c(-RGDfK-)$_4$ dose dependently slowed down the tumor growth. The mean tumor doses were 1.28 and 1.81 Gy from 37 and 74 MBq of ^{64}Cu-cyclam-RAFT-c(-RGDfK-)$_4$, respectively. Peptide dose study showed that the tumor uptake of ^{64}Cu-cyclam-RAFT-c(-RGDfK-)$_4$ dose dependently decreased at doses $\geq$1 nmol, indicating a saturation of $\alpha_V\beta_3$ with the administered therapeutic doses (1 and 2 nmol). Combined analysis of the data from tumor-bearing and tumor-free mice revealed no significant toxicity caused by 37–74 MBq of ^{64}Cu-cyclam-RAFT-c(-RGDfK-)$_4$. Our study demonstrates the therapeutic efficacy and safety of ^{64}Cu-cyclam-RAFT-c(-RGDfK-)$_4$ for $\alpha_V\beta_3$-targeted radionuclide therapy. ^{64}Cu-cyclam-RAFT-c(-RGDfK-)$_4$ would be a promising theranostic drug for cancer imaging and therapy. *Mol Cancer Ther; 15(9); 2076–85. ©2016 AACR.*

Introduction

Molecular-targeted radionuclide therapy (MTRT), which is a promising cancer treatment option, is performed by the systemic administration of a specific molecular vehicle, that is, antibody, peptide or small organic molecule that is radiolabeled with a cytocidal energy-releasing radionuclide (α- or β^--particle emitter or Auger electron emitter) to elicit a therapeutic effect on the targeted tumoral lesions (1–4). The key advantages such as rapid blood clearance, tissue penetration capability, low immunogenicity, and relatively easy and cost-effective production, have made the peptide-based MTRT more attractive as a treatment strategy with clinical–translational potential (4–6).

MTRT with radiolabeled somatostatin analogues (peptide ligands), targeting somatostatin receptor highly expressed neuroendocrine tumors, have been used in clinical practice with convincing therapeutic efficacy (6, 7). Of the candidate target molecules for MTRT, $\alpha_V\beta_3$ integrin ($\alpha_V\beta_3$) is a promising one (4, 5). It is a transmembrane glycoprotein receptor and an important cell adhesion molecule that plays important roles in tumor growth, invasion, metastasis, and angiogenesis. It is highly expressed on various types of tumor cells and activated endothelial cells during angiogenesis (8–10). The $\alpha_V\beta_3$ has been identified as a biomarker for tumor angiogenesis (a key event required for tumor growth), which makes it more attractive as a therapeutic target (11–14). Of equal importance is the well-established key structure of the cyclic pentapeptide containing a tripeptide sequence Arg-Gly-Asp (cRGD) with high specificity and affinity for the $\alpha_V\beta_3$ (15). A series of cRGD-based radiotracers have been designed, synthesized, and evaluated in *in vitro* and *in vivo* studies (5, 16, 17). Of those, some early developed ones have been in clinical trials, showing valuable results for cancer imaging (17). Meanwhile, some research groups have begun to explore the therapeutic efficiency of cRGD ligand-$\alpha_V\beta_3$ receptor—based MTRT (18–23).

We have developed a tetrameric cRGD peptide–based radiopharmaceutical ^{64}Cu-cyclam-RAFT-c(-RGDfK-)$_4$ containing 4 copies of a cRGD monomer grafted onto one side of a cyclic decapeptide scaffold named RAFT (regioselectively addressable

[1]Molecular Imaging Center, National Institute of Radiological Sciences, Chiba, Japan. [2]Département de Chimie Moléculaire-UMR CNRS 5250, Université Grenoble Alpes, Grenoble, France. [3]École Nationale Supérieure de Chimie de Montpellier, Montpellier, France.

Note: Supplementary data for this article are available at Molecular Cancer Therapeutics Online (http://mct.aacrjournals.org/).

Current address for T. Furukawa: Department of Radiological and Medical Laboratory Sciences, Nagoya University Graduate School of Medicine, Nagoya, Japan; and current address for T. Saga: Department of Diagnostic Radiology, Kyoto University Hospital, Kyoto, Japan.

Corresponding Author: Zhao-Hui Jin, National Institute of Radiological Sciences, Anagawa 4-9-1, Inage, Chiba 263-8555, Japan. Phone: 8143-382-3706; Fax: 8143-206-0818; E-mail: zhaohui@nirs.go.jp

doi: 10.1158/1535-7163.MCT-16-0040

functionalized template) and a copper chelator 1,4,8,11-tetraazacyclotetradecane (cyclam) on the other side of the RAFT (24, 25). This radiocompound possesses a greatly improved $\alpha_V\beta_3$-binding specificity and affinity as well as a high internalization capability due to the multimeric presentation of cRGD motifs (25–27), and is capable of being applied for both imaging and therapy because of the suitable half-life (12.7 hours) of copper-64 (^{64}Cu) with multiple decay modes—β^+ (17.8%) used for positron emission tomography (PET), β^- (38.4%) and Auger electron (43%) used for therapeutic radiation (28). In fact, the antitumor activities of ^{64}Cu have been reported in preclinical studies using ^{64}Cu-labeled antibody or peptide (somatostatin analogue), or the hypoxia radiotracer ^{64}Cu-ATSM (29–32). Our previous studies have demonstrated the favorable biopharmacokinetics of ^{64}Cu-cyclam-RAFT-c(-RGDfK-)$_4$ in terms of rapid blood clearance, high metabolic stability, and predominant renal excretion, and revealed the positive correlation between tumor uptake of this probe and the corresponding tumoral $\alpha_V\beta_3$ expression levels (25, 33). PET imaging showed the potential of ^{64}Cu-cyclam-RAFT-c(-RGDfK-)$_4$ for visualizing tumor angiogenesis and monitoring antiangiogenic therapy (34). Importantly, the retention of ^{64}Cu-cyclam-RAFT-c(-RGDfK-)$_4$ in kidneys (principal dose-limiting organ for peptide-based MTRT) could be significantly reduced by coinjection with renoprotective agents, the gelatin-containing solution Gelofusine (GF) and the basic amino acid L-lysine (Lys; refs. 33, 35). The current study subsequently aimed to evaluate the therapeutic potential and side effects of ^{64}Cu-cyclam-RAFT-c(-RGDfK-)$_4$ in an $\alpha_V\beta_3$-positive tumor mouse model.

Materials and Methods

Peptides and radiolabeling

Cyclam-RAFT-c(-RGDfK-)$_4$ (Fig. 1A) and chelator-unconjugated RAFT-c(-RGDfK-)$_4$ (molecular weight: 4,119.6, and 3,879.3, respectively) were synthesized as reported previously (24). ^{64}Cu was produced using a cyclotron at the National Institute of Radiological Sciences (NIRS, Chiba, Japan). ^{64}Cu-cyclam-RAFT-c(-RGDfK-)$_4$ was prepared with a specific activity of 37 MBq/nmol and a radiochemical purity of >99.5%, based on our published procedures (25, 33, 34).

Animal tumor model and $\alpha_V\beta_3$ expression

Animal procedures were approved by the Institutional Animal Care and Use Committee of NIRS. BALB/cAJcl-*nu/nu* mice (5-week-old female, CLEA Japan, Inc.) were injected subcutaneously in the right flank with 5×10^6 U87MG human glioblastoma cells (25, 33) 17 to 20 days before the experiments. Tumor mass was measured with a digital caliper. Tumor volume (mm^3) was determined using the formula $0.5 \times \text{length} \times \text{width}^2$, and the fold of change was calculated by dividing the obtained value by the initial tumor volume measured before treatment (day 0). The survival endpoint of tumor-bearing mice was determined when tumor volume exceeded 1,500 mm^3.

The $\alpha_V\beta_3$ expression in U87MG tumor cells that were used for the current study was validated in both cell culture and xenograft levels, based on our published procedures (25), which is briefly described in the Supplementary Information. It should be stated that U87MG was directly obtained from the ATCC (May 20, 2009; characterized by STR, Y-chromosome, and Q-band assays) and immediately expanded and frozen in our laboratory. Early passage cells (fewer than the cumulative 2 to 3 months of subculture after receipt) were used for all experiments.

Biodistribution assays

Experiment 1: effects of injection vehicles. Tumor-bearing mice ($n = 6$/each group) were injected (via the tail vein) with 0.185 MBq (0.005 nmol) of ^{64}Cu-cyclam-RAFT-c(-RGDfK-)$_4$ formulated in

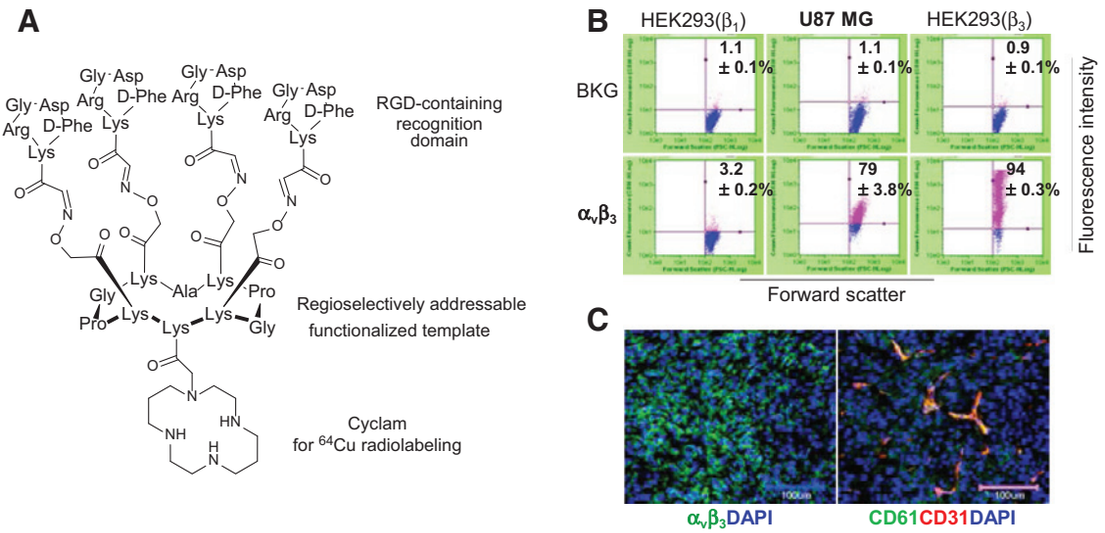

Figure 1.

A, molecular structure of cyclam-RAFT-c(-RGDfK-)$_4$. **B,** flow cytometric analysis of $\alpha_V\beta_3$ expression in U87MG cells. HEK293(β_3) and HEK293(β_1) cells were used as the positive and negative controls, respectively. The cells incubated with antibody diluent were used as the background control (BKG). Data in the top right quadrant indicate the percentage of stained cells from two or three experiments. **C,** left, immunofluorescence staining of $\alpha_V\beta_3$ expression (green) in U87MG cells in xenograft; right, endothelial $\alpha_V\beta_3$ expression (yellow) revealed by double immunofluorescence staining of CD31 (red) and CD61 (green) in U87MG xenograft. Yellow, red/green overlay. Nuclei were stained with DAPI (blue); scale bar, 100 μm.

normal saline (NS) or NS with 1% Tween 80 (NS/Tw80). At 3 hours postinjection (p.i.), the mice were sacrificed, and blood was drawn by cardiac puncture. Tumor, muscle, liver, and kidney were dissected and weighed, and radioactivity was measured using a gamma counter with decay correction. Tumor and organ uptake were presented as the percentage of injected radioactivity per gram of tissue (% ID/g) normalized to 20 g body weight.

Similar assays were performed in tumor-bearing mice ($n = 5$/each group) that received 0.74 MBq (0.02 nmol) of ^{64}Cu-cyclam-RAFT-c(-RGDfK-)$_4$ formulated in NS/Tw80 or NS/Tw80 supplemented with GF (80 mg/kg; Braun Medical) and Lys (400 mg/kg; Sigma-Aldrich; NS/Tw80/GF/Lys; ref. 33). GF, consisting of a 40 g/L solution of succinylated gelatin, was a kind gift from Lucie Sancey (University of Lyon 1, France).

Experiment 2: effects of peptide doses. Tumor-bearing mice ($n = 4$–5) were injected with 0.74 MBq of ^{64}Cu-cyclam-RAFT-c(-RGDfK-)$_4$ in NS/Tw80/GF/Lys injection vehicle added with varying amounts of unlabeled cyclam-RAFT-c(-RGDfK-)$_4$ to give final injectates at ascending doses of 0.25, 0.5, 1, 2, 4, and 10 nmol. The effects of peptide doses on the tumor and organ tracer uptake were evaluated at 3 hours p.i.

Experiment 3: chronologic changes at therapeutic doses. The biodistribution data of 74 MBq (2 nmol) of ^{64}Cu-cyclam-RAFT-c(-RGDfK-)$_4$ was obtained from tumor-bearing mice ($n = 5$–6) that were injected with 0.74 MBq of ^{64}Cu-cyclam-RAFT-c(-RGDfK-)$_4$ in NS/Tw80/GF/Lys injection vehicle, with the peptide dose adjusted to 2 nmol by adding the unlabeled cyclam-RAFT-c(-RGDfK-)$_4$. Tumor and major organ uptakes were determined at 2, 5, 10, and 20 minutes, and at 1, 3, and 24 hours p.i. By assuming that the tumor or normal tissue uptake ratio of 1 nmol (corresponding to 37 MBq) to 2 nmol (corresponding to 74 MBq) of ^{64}Cu-cyclam-RAFT-c(-RGDfK-)$_4$ at 3 hours p.i. (TUR), which could be calculated from the results of Experiment 2, are similar to those at other time-points, the time course of 37 MBq of ^{64}Cu-cyclam-RAFT-c(-RGDfK-)$_4$ biodistribution data were extrapolated by multiplying the % ID/g obtained with the dose of 0.74 MBq (2 nmol) with the corresponding TUR.

Therapy experiments

Four groups of tumor-bearing mice ($n = 6$–8) were injected with NS/Tw80 (vehicle control), 1 nmol of RAFT-c(-RGDfK-)$_4$ (peptide control), or 37 MBq (1 nmol) of ^{64}Cu-cyclam-RAFT-c(-RGDfK-)$_4$ with or without GF/Lys (± GF/Lys). In the second set of therapy study, 4 groups of tumor-bearing mice ($n = 9$–10) received NS/Tw80/GF/Lys (vehicle control), 2 nmol of RAFT-c(-RGDfK-)$_4$, 37 MBq (1 nmol) or 74 MBq (2 nmol) of ^{64}Cu-cyclam-RAFT-c(-RGDfK-)$_4$. After injections, mouse body weight (g) and tumor size were measured every 2 days, and survival endpoint days were recorded.

Hematology and hepatorenal functions

For all groups of mice involved in the therapy experiments, routine peripheral blood tests were performed at days 3, 7, and 12 p.i. as well as on their survival endpoint days, whereas the routine hepatorenal function test was performed only on the survival endpoint day due to the limitation of blood collection. For detailed procedures, see Supplementary Information.

Side effects were also studied in 2 groups of tumor-free mice ($n = 4$/each group, at the same age as the tumor-bearing mice used for the therapy study) that received administration of NS/Tw80/GF/Lys vehicle and 74 MBq of ^{64}Cu-cyclam-RAFT-c(-RGDfK-)$_4$, respectively. The survival endpoint was determined on the basis of the mean survival day of 74-MBq-treated tumor-bearing mice.

Autoradiography and histologic studies

Tumor-bearing mice were injected with the therapeutic dose of 74 MBq (2 nmol) of ^{64}Cu-cyclam-RAFT-c(-RGDfK-)$_4$, and sacrificed at 3 hours p.i. Autoradiographic examination, hematoxylin and eosin (H&E) staining, and immunofluorescence staining of the tumor microvasculature and $\alpha_V\beta_3$ expressed by the tumor cells were performed on the serial frozen sections of the excised tumor. The procedures, based on our published methods (34), are briefly described in the Supplementary Information.

As a separate experiment, tumors ($n = 4$/each group at each time point) were sampled at days 1, 3, and 6 p.i. of NS/Tw80/GF/Lys vehicle or 74 MBq of ^{64}Cu-cyclam-RAFT-c(-RGDfK-)$_4$, which was followed by immunohistochemical staining for proliferation (Ki67), apoptosis (TUNEL assay), and microvessels (CD31). See the Supplementary Information for the detailed procedures.

Radiation dosimetry

The absorbed doses in the tumor and normal tissues of the mice treated with 37 (1 nmol) or 74 MBq (2 nmol) of ^{64}Cu-cyclam-RAFT-c(-RGDfK-)$_4$ were calculated on the basis of the time course of biodistribution data of ^{64}Cu-cyclam-RAFT-c(-RGDfK-)$_4$ at corresponding doses as well as the mean energy emitted per transition (MEEPT) of ^{64}Cu, 1.22×10^{-14} Gy kg (Bq s)$^{-1}$ (β^-, 97.4%; Auger electron, 2.6%; ref. 36). From the biodistribution data, the tumor and organ time–activity curves were plotted and the AUCs were calculated for representing the residence time of the injected radiocompound. The absorbed doses were calculated according to the formula AUC × MEEPT × injected activity (37).

Statistical analysis

Quantitative data were presented as mean ± SD. The unpaired t test was used for two groups' comparison, and one-way ANOVA followed by the Dunnett test for multiple comparisons (KaleidaGraph Version 4.0, Synergy Software). On the basis of the period from day 0 p.i. to the specified survival endpoint day, Kaplan–Meier survival curves were plotted using KaleidaGraph, and the mean survival days were compared. P values <0.05 were considered statistically significant.

Results

$\alpha_V\beta_3$ expression in U87MG cell culture and xenograft

Flow cytometric analysis (Fig. 1B) demonstrated the expression of $\alpha_V\beta_3$ in nearly 80% of the examined U87MG cells. Immunofluorescence staining of U87MG xenograft showed positive expression of $\alpha_V\beta_3$ in the majority of tumor cells (Fig. 1C, left), whereas the cells double-stained for the panendothelial marker CD31 and mouse CD61 (integrin β_3 subunit) were identified as the $\alpha_V\beta_3$-positive neoendothelial cells (Fig. 1C, right).

Effects of injection vehicles on ^{64}Cu-cyclam-RAFT-c(-RGDfK-)$_4$ biodistribution

Cyclam-RAFT-c(-RGDfK-)$_4$ with low water solubility was dissolved in dimethyl sulfoxide and labeled with ^{64}Cu. Previously, ^{64}Cu-labeled cyclam-RAFT-c(-RGDfK-)$_4$ was diluted in NS just before *in vivo* use. On the basis of the results of solubility test

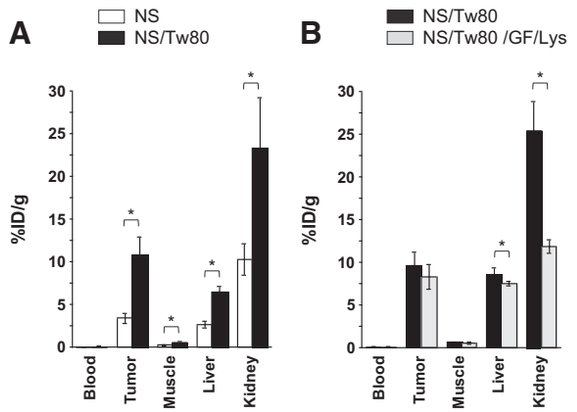

Figure 2.

Effects of injection vehicles on ^{64}Cu-cyclam-RAFT-c(-RGDfK-)$_4$ biodistribution in U87MG tumor-bearing mice at 3 hours p.i. **A,** ^{64}Cu-cyclam-RAFT-c(-RGDfK-)$_4$ (0.185 MBq, 0.005 nmol) formulated in NS and NS/Tw80, respectively. **B,** ^{64}Cu-cyclam-RAFT-c(-RGDfK-)$_4$ (0.74 MBq, 0.02 nmol) formulated in NS/Tw80 ± GF/Lys; *, $P < 0.05$.

conducted earlier (unpublished data), in the current study, Tw80 (a pharmaceutical excipient) was added to the injectate for solubility improvement. As shown in Fig. 2A, the addition of 1% Tw80 to the NS-vehicle led to a markedly increased tumor uptake from 3.4 ± 0.61% ID/g to 10.8 ± 0.86% ID/g at 3 hours p.i. Moreover, the tumor-to-blood ratio was significantly higher with NS/Tw80-vehicle than with NS-vehicle (158 ± 37 vs. 102 ± 38, $P = 0.025$). The tumor-to-muscle ratio with NS/Tw80-vehicle was slightly higher than that with NS-vehicle (18.8 ± 2.5 vs. 16.7 ± 4.4, $P > 0.05$). However, the kidney uptake was unfavorably elevated with the use of NS/Tw80-vehicle (Fig. 2A). With the addition of GF and Lys, which were previously reported to markedly reduce the renal uptake and slightly increase the tumor uptake of ^{64}Cu-cyclam-RAFT-c(-RGDfK-)$_4$ (33), the high renal uptake caused by NS/Tw80 was greatly reduced by 54%, whereas no significant difference was found with the tumor uptake values (Fig. 2B).

Radiotherapy with ^{64}Cu-cyclam-RAFT-c(-RGDfK-)$_4$

The treatment outcomes of mice that received single administration of 37 MBq (1 nmol) of ^{64}Cu-cyclam-RAFT-c(-RGDfK-)$_4$ ± GF/Lys are shown in Supplementary Fig. S1; Supplementary Tables S1 and S2. ^{64}Cu-cyclam-RAFT-c(-RGDfK-)$_4$ ± GF/Lys, but not the unlabeled peptide, similarly induced a significant delay of tumor growth as compared with the NS/Tw80-vehicle control (Supplementary Fig. S1A). It was observed that without GF/Lys coinjection, the mice treated with ^{64}Cu-cyclam-RAFT-c(-RGDfK-)$_4$ had significantly lower body weight on days 3 and 6 as compared with the vehicle control mice (Supplementary Fig. S1C), and GF/Lys did not seem to greatly alter hematologic and hepatorenal functions compared with the compound alone (37 MBq vs. 37 MBq + GF/Lys; Supplementary Fig. S1D–S1E and Supplementary Tables S1 and S2). On the basis of these results, ^{64}Cu-cyclam-RAFT-c(-RGDfK-)$_4$ formulated in the vehicle of NS/Tw80/GF/Lys was used for all subsequent studies.

The treatment outcomes of mice that received single administration of increasing dose of ^{64}Cu-cyclam-RAFT-c(-RGDfK-)$_4$ are summarized in Fig. 3, Table 1, and Supplementary Table S3. No significant difference was found in the initial tumor volumes (mean values ranging from 89 to 96 mm^3) among the 4 groups of mice. The administration of 2 nmol of RAFT-c(-RGDfK-)$_4$ did not significantly influence the tumor growth as compared with the vehicle control (Fig. 3A). As compared with 37 MBq (1 nmol), the treatment with 74 MBq (2 nmol) of ^{64}Cu-cyclam-RAFT-c(-RGDfK-)$_4$ resulted in an improved tumor growth inhibition (Fig. 3A); at day 12 p.i., the fold change in tumor volume was 4.96 ± 2.79 ($P = 0.011$) and 6.96 ± 2.73 ($P = 0.236$) for 74-MBq- and 37-MBq–treated mice, respectively, versus 9.36 ± 4.05 for the vehicle control mice. Furthermore, significantly prolonged survival endpoint days were achieved in 74-MBq–treated mice (20 ± 3.2 days vs. 16.4 ± 3.4 days for the vehicle control, $P = 0.013$; Fig. 3B). All groups of mice showed similar body weight gains with no significant difference (Fig. 3C). Significantly, decreased white blood cell count (WBC) was found in 74-MBq- and 37-MBq–treated mice on days 7 and 12 (Fig. 3D; Supplementary Table S3). Except for this, the red blood cell count (RBC; Fig. 3E), the platelet count (PLT; Fig. 3F), and the measurements of hemoglobin, hematocrits, and red blood cell indices (data not shown) did not indicate hematologic toxicity. The results of hepatorenal functions (Table 1) showed slightly elevated levels of creatinine (CRE) and gamma-glutamyl transpeptidase (GGT) in 74-MBq–treated mice on their survival endpoints.

Supplementary Fig. S2 and Supplementary Table S4 show the results of toxicity studies performed in tumor-free mice. As compared with the vehicle control, 74 MBq of ^{64}Cu-cyclam-RAFT-c(-RGDfK-)$_4$ induced a 26.5% decrease in WBCs (2,300 ± 410/μL vs. 3130 ± 460/μL; $P = 0.037$) and a 21.8% increase in PLTs (59.5 ± 4.1 ×10^4/μL vs. 72.5 ± 8.8 ×10^4/μL; $P = 0.036$) at day 3 p.i., both of which then recovered to the control levels by day 7 p.i. Except for these, no other significant alterations were detected.

Autoradiography and histologic studies

Autoradiographic examination (Fig. 4A) indicates a relatively heterogeneous intratumoral distribution of ^{64}Cu-cyclam-RAFT-c(-RGDfK-)$_4$. H&E staining (Fig. 4B) did not show obvious necrosis in the examined tumor. Figure 4C depicts the staining pattern of $\alpha_V\beta_3$ on tumor cells, which was overlapped with the radioactive distribution (Fig. 4A). CD31 staining (Fig. 4D) showed that the tumor microvasculature was quite homogeneous with high capillary density. The findings of H&E and CD31 staining may exclude the relation of the relatively weak radioactivity accumulation with the necrosis and poor blood supply.

The results of time course of histologic analysis of the 74-MBq–treated tumors are presented in Fig. 5. Ki67 staining revealed a significantly reduced proliferation index (the percentage of Ki67-positive cells) at day 1 p.i. for treated tumors as compared with the vehicle control, which tended to maintain at least until day 6 (Fig. 5B). For microvessel density (MVD) as determined by CD31 staining, a significant decrease was found at the later time point of day 6 in treated tumors as compared with the control (Fig. 5C). TUNEL staining detected generally low levels of apoptosis for both treated and vehicle control tumors at all time-points (days 1, 3, and 6), but it was also found that at day 6 the DNA fragmentation and apoptosis seemed to slightly increase in treated tumors (Fig. 5A, right).

Biodistribution and radiation dosimetry studies

The biodistribution results of 0.74 MBq of ^{64}Cu-cyclam-RAFT-c(-RGDfK-)$_4$ with ascending peptide doses of 0.25 to 10 nmol at 3 hours p.i. are shown in Fig. 6A. The tumor uptake was

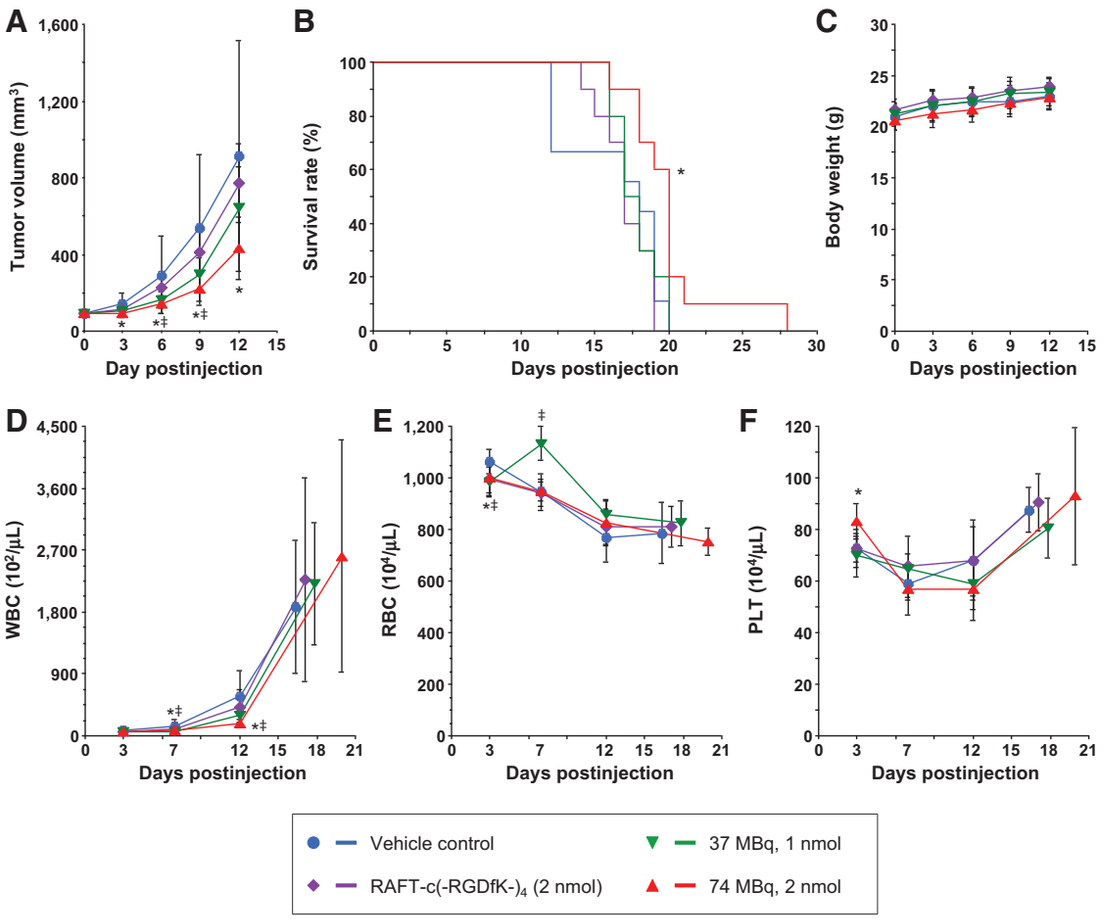

Figure 3.

Radiotherapy with increasing doses of ^{64}Cu-cyclam-RAFT-c(-RGDfK-)$_4$. U87MG tumor-bearing mice were injected with NS/Tw80/GF/Lys (vehicle control), 2 nmol of RAFT-c(-RGDfK-)$_4$, or 37 MBq (1 nmol) or 74 MBq (2 nmol) of ^{64}Cu-cyclam-RAFT-c(-RGDfK-)$_4$. **A,** tumor growth curves. **B,** Kaplan–Meier survival curves. **C,** time course of body weight. **D–F,** time course of WBCs, RBCs, and PLTs (**D, E,** and **F,** respectively). The final data points shown in **D–F** represent the results obtained at survival endpoint days (as presented by a mean value). *, $P < 0.05$ for 74 MBq-group versus vehicle control; ‡, $P < 0.05$ for 37 MBq-group versus vehicle control.

7.1 ± 1.0% ID/g at 0.25 nmol, which was significantly decreased at doses ≥ 1 nmol in a dose-dependent manner (4.8 ± 0.35, 3.4 ± 0.23, 2.2 ± 0.22, and 1.2 ± 0.16% ID/g for 1, 2, 4, and 10 nmol, respectively). Except for the kidney, similar dose responses were observed in other normal tissues examined. The highest uptake was found in kidney, followed by liver and tumor. As compared with liver, the tracer uptake by the $\alpha_v\beta_3$-positive tumor was more affected. A 40-fold increase of peptide dose from 0.25 to 10 nmol induced 83.5% reduction in the tumor uptake versus 52.1% reduction in the liver uptake.

Time course of 0.74 MBq of ^{64}Cu-cyclam-RAFT-c(-RGDfK-)$_4$ biodistribution is presented in Fig. 6B, which most likely represents the biopharmacokinetics of ^{64}Cu-cyclam-RAFT-c(-RGDfK-)$_4$ when used for 74 MBq-radiotherapy because the same peptide

Table 1. Effects of 74 MBq (2 nmol) of ^{64}Cu-cyclam-RAFT-c(-RGDfK-)$_4$ + GF/Lys on hepatorenal functions of U87MG tumor-bearing mice

	Liver enzyme values (U/L)				Renal function indices (mg/dL)	
Group of mice	**GOT**	**GPT**	**GGT**	**ALP**	**CRE**	**BUN**
NS/Tw80/GF/Lys (vehicle)	116 ± 26	28 ± 7.1	5.9 ± 1.5	116 ± 15	0.30 ± 0.05	21 ± 2.7
RAFT-c(-RGDfK-)$_4$ (2 nmol)	131 ± 46	42 ± 30	6.9 ± 2.8	116 ± 17	0.28 ± 0.13	21 ± 3.6
^{64}Cu-cyclam-RAFT-c(-RGDfK-)$_4$ (37 MBq, 1 nmol)	148 ± 28	42 ± 13	8.3 ± 3.1	108 ± 6.6	0.30 ± 0.15	21 ± 2.9
^{64}Cu-cyclam-RAFT-c(-RGDfK-)$_4$ (74 MBq, 2 nmol)	156 ± 62[a]	66 ± 49[b]	9.1 ± 3.3[c]	122 ± 34	0.50 ± 0.21[c]	24 ± 4.3

NOTE: Mice were sacrificed when tumor grew beyond 1,500 mm^3, and the blood was sampled and assessed. The data are presented as mean ± SD (n = 9–10).
[a]n = 9 (the exceptionally high value of 452 U/L in the tenth mouse was omitted).
[b]n = 9 (the exceptionally high value of 525 U/L in the tenth mouse was omitted).
[c]$P < 0.05$ versus vehicle control.

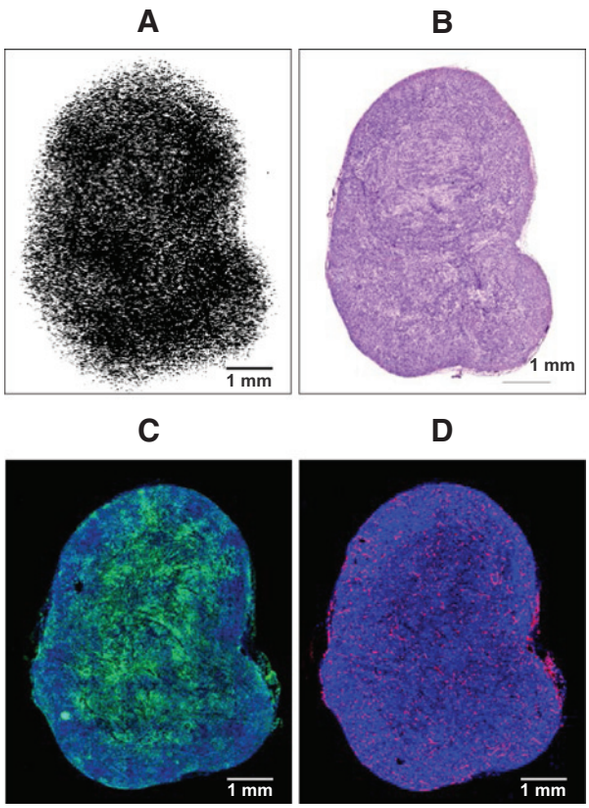

Figure 4.

A, autoradiograph of ^{64}Cu-cyclam-RAFT-c(-RGDfK-)$_4$ distribution in a whole-tumor section at 3 hours p.i. **B–D,** H&E staining (**B**) and immunofluorescence staining of $\alpha_V\beta_3$ expressed by the tumor cells (**C,** green) as well as the tumor microvasculature using the panendothelial marker CD31 (**D,** red) on the serial sections. Nuclei were stained with DAPI (blue); scale bar, 1 mm.

dose of 2 nmol was used. This radiopharmaceutical had rapid blood clearance, rapid and high tumor uptake, and predominant renal excretion. The tumor uptake was 3.8 ± 0.39% ID/g at 1 hour p.i., which was maintained at 3.4 ± 0.58% ID/g at 24 hours p.i. Table 2 lists the absorbed doses in tumor and other organs from 37 and 74 MBq of ^{64}Cu-cyclam-RAFT-c(-RGDfK-)$_4$ calculated on the basis of the methods described in the Materials and Methods. The highest absorbed dose was received by the kidneys and followed by the liver and tumor in both 37- and 74-MBq–treated mice. As compared with radiotherapy with 37 MBq of ^{64}Cu-cyclam-RAFT-c(-RGDfK-)$_4$, 2-fold increase in the administered radioactivity dose (74 MBq) resulted in 1.4-, 1.9-, and 2.0-fold increases in the absorbed doses for the tumor, the liver, and the kidney, respectively.

Discussion

There is a growing interest in evaluating the therapeutic potential of cRGD peptide–based radiopharmaceuticals. In the previously published works (18–23), cRGD-monomer, -dimer or -tetramer was labeled with yttrium-90 (^{90}Y, half-life 2.7 days) or lutetium-177 (^{177}Lu, half-life 6.7 days), the most 2 common β^--emitting radionuclides employed for MTRT. Single or fractionated dose injection of these radiocompounds with total activities of 33.3−37 MBq for ^{90}Y and 37−222 MBq for ^{177}Lu caused tumor growth delay in various $\alpha_V\beta_3$-positive tumor mouse models. The current study showed that single dose administrations of 37 and 74 MBq of the PET probe ^{64}Cu-cyclam-RAFT-c(-RGDfK-)$_4$ could also induce tumor growth delay in the established $\alpha_V\beta_3$-positive U87MG tumor mouse model. To our knowledge, this is the first report demonstrating the therapeutic potential of ^{64}Cu-labeled cRGD peptide.

Tumor-absorbed dose (TAD) is an important parameter correlating with the biological response of tumor during radiotherapy. However, a wide range of TADs, 17−11171 mGy/MBq or 0.019−187 Gy, were described in a review of MTRT using a variety of antibodies labeled with various radionuclides in animals bearing various types of human tumor xenografts (38). Even in similar tumor (colon cancer) animal models, the mean TADs ranged widely from 3.3 to 72 Gy (29). It was suggested that when evaluating the tumor response, in addition to TAD, many factors such as tumor dimension, vascularization, radiosensitivity, activity distribution, and so on, should be considered (29, 38). In a rat therapy study using ^{64}Cu-labeled peptide analogue of somatostatin, the estimated TADs between 4.7−5.4 Gy were reported to give significant tumor growth inhibition (30). As for the therapy studies using ^{177}Lu or ^{90}Y-labeled cRGD peptides in similar U87MG tumor models, no TAD was reported (22, 23). The current study showed mean TADs of 1.28 Gy (34.6 mGy/MBq) and 1.81 Gy (24.4 mGy/MBq) from 37 and 74 MBq of ^{64}Cu-cyclam-RAFT-c(-RGDfK-)$_4$, respectively. The doses of 1.28–1.81 Gy are, indeed, relatively low, but brought the growth-inhibitory effect on the U87MG glioblastoma. Other factors possibly contributing to the antitumor activities of ^{64}Cu-cyclam-RAFT-c(-RGDfK-)$_4$ should be taken into account. As demonstrated by the histologic analyses of the tumors treated with 74 MBq of ^{64}Cu-cyclam-RAFT-c(-RGDfK-)$_4$ (Fig. 5), besides the inhibition of tumor cell proliferation, the cytocidal radiation was effective against $\alpha_V\beta_3$-positive neoendothelial cells also, which was revealed by a significant decrease in MVD achieved at day 6 posttreatment. In our preliminary study (Supplementary Fig. S3), CD31 staining of U87MG tumors excised at day 13 p.i. of 37 MBq of ^{64}Cu-cyclam-RAFT-c(-RGDfK-)$_4$ showed a reduced MVD and also indicated sparse formation of endothelial cell connections in comparison with the network-like structures of endothelial cells observed in vehicle-treated tumors. Similar findings were reported by other groups using ^{177}Lu-labeled cRGD peptide (22) or ^{90}Y-labeled anti-$\alpha_V\beta_3$ antibody (39). Furthermore, for the targeted cells, both cell membrane and intracellular substructures would be damaged because of the binding of ^{64}Cu-cyclam-RAFT-c(-RGDfK-)$_4$ to the cell membrane–localized $\alpha_V\beta_3$ as well as its potential for efficient cell internalization (26, 27). Correspondingly, the possibility of contribution from the Auger electron emission of the internalized ^{64}Cu (low energy, but high linear energy transfer) on the DNA damage should be borne in mind. An additional consideration could be about the intratumoral inhomogeneous radioactivity distribution, which indicates that a proportion of tumor cells might receive much higher absorbed doses than the calculated mean value, and the cytocidal effects on these cells would considerably contribute to the tumor growth inhibition.

Side effects evaluation was made in terms of body weight, hematology, and hepatorenal functions. For all groups of mice that received single administrations of 37 MBq (± GF/Lys) and 74 MBq (+ GF/Lys) of ^{64}Cu-cyclam-RAFT-c(-RGDfK-)$_4$, no

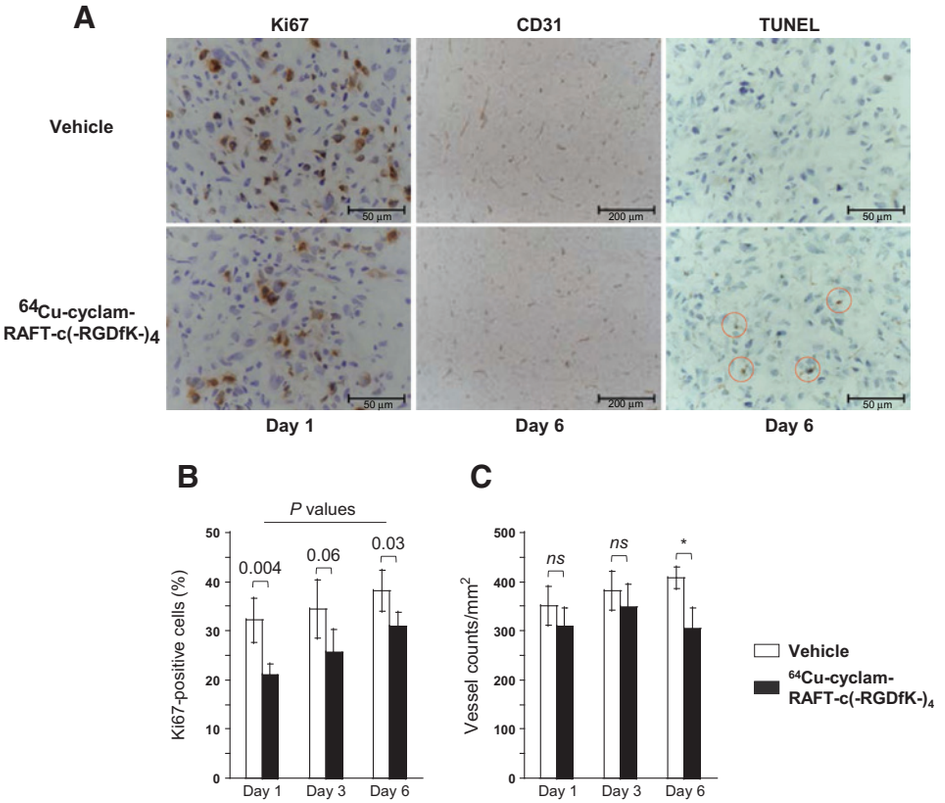

Figure 5.
Ki67, CD31, and TUNEL staining (dark brown) of the frozen tumor sections at days 1, 3, and 6 p.i. of NS/Tw80/GF/Lys vehicle or 74 MBq of ^{64}Cu-cyclam-RAFT-c(-RGDfK-)$_4$. **A,** representative images. Scale bar, 50 μm for Ki67 and TUNEL, 200 μm for CD31. Nuclei were lightly stained with hematoxylin (blue). Dotted circles indicate positively stained cells. **B,** quantitative analysis of Ki67 staining (the percentage of positively stained cells). **C,** MVD quantification (vessel counts/mm^2). ns, $P > 0.05$; *, $P < 0.05$.

significant side effect was indicated by the body weight change. In the hematologic examination performed in 74-MBq–treated normal mice, except for the transiently decreased WBCs and increased PLTs (both on day 3), no other significant alterations were detected, indicating the limited hematologic reaction. For tumor-bearing mice, we noticed that WBCs increased in line with the tumor growth (Fig. 3A and D; Supplementary Fig. S1A and S1D). Supplementary Fig. S4 shows a strong and positive correlation between the tumor volume and the corresponding WBCs in vehicle control groups. This phenomenon may be considered as the tumor-associated granulocytosis (the presence of excessive granulocytes, a category of white blood cells, in peripheral blood). As a paraneoplastic syndrome, granulocytosis occurs in a proportion of patients with various types of solid tumor, including glioblastoma (40, 41), and the WBCs of a cancer patient with granulocytosis could be normalized after chemo- or radiotherapy, and again increased with the recurrence (41). On the basis of these, the lower WBCs detected in 37- or 74-MBq–treated tumor-bearing mice at day 7 and/or 12 p.i. were most probably due to the tumor cell proliferation inhibition caused by ^{64}Cu-cyclam-RAFT-c(-RGDfK-)$_4$. As for the blood biochemical parameters of hepatorenal functions, statistically significant findings were found in 74-MBq–treated tumor-bearing mice on their survival endpoint days (20 ± 3.2 days), with somewhat elevated levels of CRE (indicating a decrease in glomerular filtration rate) and GGT (suggesting liver damage). Subsequent examination of 74-MBq–treated normal mice did not show any significant alteration 20 days p.i. (the same time period of the mean survival day of 74-MBq-treated tumor-bearing mice). Thus, we considered that the potential toxicity of ^{64}Cu-cyclam-RAFT-c(-RGDfK-)$_4$ to liver (mean absorbed dose of 3.70 Gy) and kidneys (mean absorbed dose of 5.27 Gy) would be negligible. In fact, the CRE value of 0.50 ± 0.21 mg/dL (equal to 44.2 ± 18.6 μmol/L) in the group of tumor-bearing mice treated with 74 MBq of ^{64}Cu-cyclam-RAFT-c(-RGDfK-)$_4$ (Table 1) are lower than the reported values of 67.8 ± 12 and 86.6 ± 23 μmol/L obtained with similar therapeutics using 37 MBq of ^{177}Lu- and ^{90}Y-labeled analogues, respectively (23).

As mentioned, the therapeutic doses of 37 and 74 MBq contained 1 and 2 nmol of cyclam-RAFT-c(-RGDfK-)$_4$, respectively, which are however not yet the most optimal dosing because the peptide dose escalation studies (Fig. 6A, 0.25–10 nmol; Supplementary Fig. S5, 0.005–0.5 and 10 nmol) revealed significantly reduced tumor uptake at such doses, most likely due to saturation of the $\alpha_V\beta_3$ receptor. The saturable peptide uptake was also reported by other investigators (19, 42). We found that increasing the administered activity of ^{64}Cu-cyclam-RAFT-c(-RGDfK-)$_4$ from 37 to 74 MBq led to only a 1.41-fold higher TAD and somewhat enhanced antitumor effects. Approaches for avoiding saturation-caused decrease of tumor uptake would lead to an improved therapeutic efficacy of ^{64}Cu-cyclam-RAFT-c(-RGDfK-)$_4$. One way is to enhance the specific activity of ^{64}Cu-cyclam-RAFT-c(-RGDfK-)$_4$, which would be achieved by improving the specific radioactivity and purity of $^{64}CuCl_2$ produced, optimizing the labeling and purification protocols, and/or modifying the peptide itself. Another possible strategy is to perform rapid dose fractionation as advocated by Janssen and colleagues who reported a higher tumor uptake achieved by the administration of 5.0 μg dose of 37 MBq of ^{90}Y-labeled cRGD-peptide dimer in five equal portions (1 or 2 hours apart), as compared with the single dose administration (42). It may be necessary to mention that the conventional dose

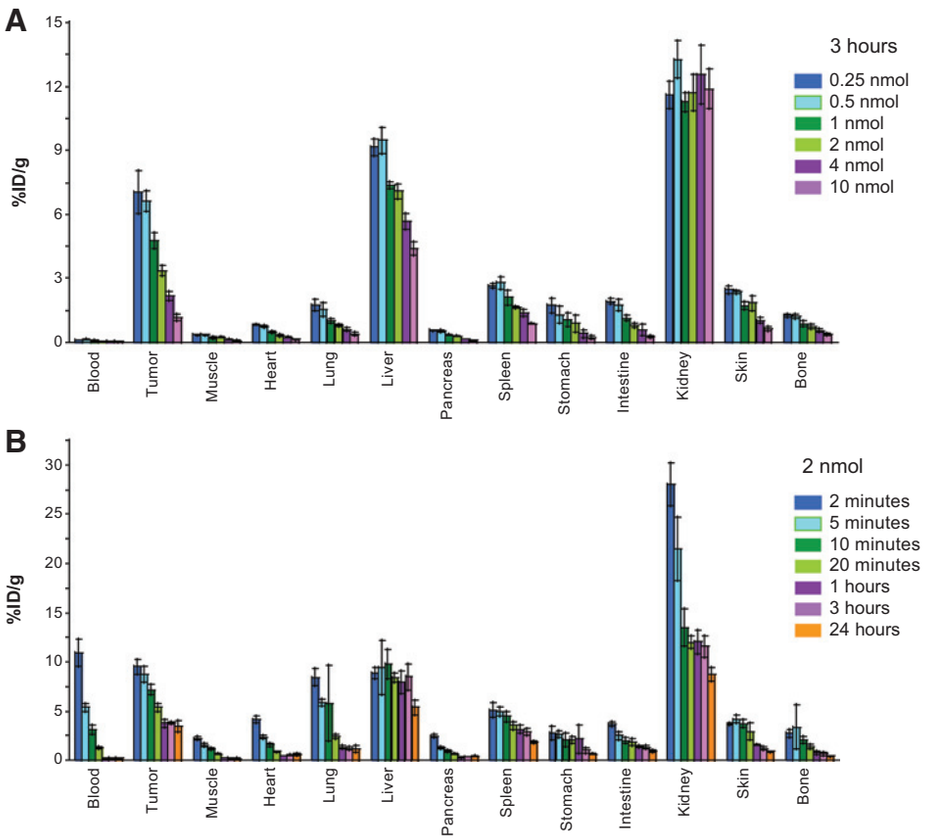

Figure 6.
A, biodistribution of 0.74 MBq of ^{64}Cu-cyclam-RAFT-c(-RGDfK-)$_4$ at various indicated peptide doses in U87MG tumor-bearing mice at 3 hours p.i. **B,** time course of biodistribution of 0.74 MBq (2 nmol) of ^{64}Cu-cyclam-RAFT-c(-RGDfK-)$_4$ in U87MG tumor-bearing mice at various indicated time points postinjection.

fractionating strategy is performed by injecting a totally high activity dose in much longer time intervals (a couple of days apart), which may improve the treatment efficacy by altering the tumor growth pattern, and reduce the potential radiation toxicity to normal tissues.

Human dosimetry was extrapolated from the biodistribution data of ^{64}Cu-cyclam-RAFT-c(-RGDfK-)$_4$ (+ GF/Lys) in tumor-bearing mice (see details in Supplementary Table S5). The mean whole body effective dose of 0.030 mSV/MBq is similar to 0.031 mSV/MBq (estimated from rat data) for ^{177}Lu-labeled somatostatin analogue peptide DOTA-TATE (a clinical radiotherapeutic agent; ref. 43), and lower than 0.111–0.114 mSV/MBq (estimated from mouse data) for ^{90}Y-labeled RAFT-c(-RGDfK-)$_4$ (23). For the kidneys, the major dose-limiting organs for MTRT, the mean absorbed dose of 0.058 mGy/MBq is more than 10 times lower than the value of 0.670 mGy/MBq for ^{177}Lu-DOTA-TATE (43). The results of human absorbed dose estimation may indicate that MTRT with ^{64}Cu-cyclam-RAFT-c(-RGDfK-)$_4$ would be safe for human use.

Table 2. Mouse mean absorbed doses calculated on the basis of the biodistribution results of ^{64}Cu-cyclam-RAFT-c(-RGDfK-)$_4$ in U87MG tumor-bearing mice

	^{64}Cu-cyclam-RAFT-c(-RGDfK-)$_4$	
	74 MBq	37 MBq
Organ	Gy (mGy/MBq)	
Blood	0.141 (1.91)	0.077 (2.08)
Tumor	1.805 (24.4)	1.280 (34.6)
Muscle	0.105 (1.42)	0.053 (1.43)
Heart	0.268 (3.62)	0.189 (5.11)
Lung	0.620 (8.38)	0.392 (10.6)
Liver	3.695 (49.9)	1.920 (51.9)
Pancreas	0.181 (2.45)	0.106 (2.86)
Spleen	1.290 (17.4)	0.824 (22.3)
Stomach	0.510 (6.89)	0.298 (8.05)
Intestine	0.604 (8.16)	0.425 (11.5)
Kidney	5.273 (71.3)	2.537 (68.6)
Skin	0.597 (8.07)	0.279 (7.54)
Bone	0.323 (4.36)	0.188 (5.08)

Including the present study, cRGD peptides labeled with either of ^{90}Y, ^{177}Lu, or ^{64}Cu have shown therapeutic potential as a MTRT radiopharmaceutical. Making a comparison of the efficacy of these radiocompounds may be difficult because each radionuclide has its unique physical properties, and each radiocompound was evaluated in a different experimental setting. Generally, ^{90}Y-cRGD peptides are optimal for large tumors because ^{90}Y is a high-energy β^- emitter (maximum energy, E_{max}: 2.28 MeV) with a longer penetration path-length in tissue (maximum length, R_{max}: ~11.3 mm; ref. 44). ^{177}Lu- or ^{64}Cu-cRGD peptides are considered more appropriate for small tumoral lesions or micrometastases due to the low-energy β^- emitters of ^{177}Lu (E_{max} 0.497 MeV, 78.7%; R_{max} 2 mm) and ^{64}Cu (E_{max} 0.573 MeV, 38.4%; R_{max} 2.5 mm; ref. 44). Another important issue considered for MTRT is the individualized dosimetry for patient selection and dosing schedule, which can be directly performed by SPECT (^{177}Lu) and PET (^{64}Cu) without using a radionuclide surrogate, with the latter being superior to the former in both sensitivity and spatial resolution. However, for ^{90}Y (a pure β^- emitter)-cRGD peptide, a suitable surrogate tracer is needed. Finally, it may be interesting to mention about the typical therapeutic copper radioisotope of

^{67}Cu (half-life 2.58 days). With a mean β^- energy of 0.141 MeV and a mean penetration path-length of 0.2 mm, ^{67}Cu-radiocompounds are considered more appropriate for the treatment of small tumors $\leq$5 mm in diameter (44, 45). We have confirmed the radiolabeling of cyclam-RAFT-c(-RGDfK-)$_4$ with ^{67}Cu using the same procedure for preparing ^{64}Cu-cyclam-RAFT-c(-RGDfK-)$_4$ for future therapy study.

In conclusion, this study provides the first evaluation of the potential of ^{64}Cu-labeled cRGD peptide for $\alpha_V\beta_3$-targeted radionuclide therapy. Single-dose administrations of 37 and 74 MBq of ^{64}Cu-cyclam-RAFT-c(-RGDfK-)$_4$ dose dependently induced tumor growth delay in the widely used $\alpha_V\beta_3$-positive U87MG tumor mouse model, without causing considerable toxicities. Improved therapeutic efficacy can be expected through circumventing the receptor saturation. ^{64}Cu-cyclam-RAFT-c(-RGDfK-)$_4$ would be a promising theranostic drug for cancer imaging and therapy.

Disclosure of Potential Conflicts of Interest

No potential conflicts of interest were disclosed.

Authors' Contributions

Conception and design: Z.-H. Jin, T. Furukawa, D. Boturyn, P. Dumy, T. Saga
Development of methodology: Z.-H. Jin
Acquisition of data (provided animals, acquired and managed patients, provided facilities, etc.): Z.-H. Jin, M. Degardin, A.B. Tsuji, T. Yamasaki, M.-R. Zhang
Analysis and interpretation of data (e.g., statistical analysis, biostatistics, computational analysis): Z.-H. Jin, M. Degardin, A.B. Tsuji, T. Yamasaki
Writing, review, and/or revision of the manuscript: Z.-H. Jin, T. Furukawa, M. Degardin, A.B. Tsuji, D. Boturyn, T. Saga
Administrative, technical, or material support (i.e., reporting or organizing data, constructing databases): A. Sugyo, K. Kawamura, Y. Fujibayashi, M.-R. Zhang
Study supervision: T. Furukawa, T. Saga

Acknowledgments

We would like to thank the Molecular Probe Program (NIRS) for supplying the ^{64}Cu produced for this study and the Cyclotron Operation Section for cyclotron operation, and our colleagues for the precious advice on this work.

The costs of publication of this article were defrayed in part by the payment of page charges. This article must therefore be hereby marked *advertisement* in accordance with 18 U.S.C. Section 1734 solely to indicate this fact.

Received January 26, 2016; revised May 20, 2016; accepted June 20, 2016; published OnlineFirst July 15, 2016.

References

1. Perkins A. *In vivo* molecular targeted radiotherapy. Biomed Imaging Interv J 2005;1:e9.
2. Larson SM, Krenning EP. A pragmatic perspective on molecular targeted radionuclide therapy. J Nucl Med 2005;46:1S–3S.
3. Pouget JP, Lozza C, Deshayes E, Boudousq V, Navarro-Teulon I. Introduction to radiobiology of targeted radionuclide therapy. Front Med 2015;2:12.
4. Dash A, Chakraborty S, Pillai MR, Knapp FF Jr. Peptide receptor radionuclide therapy: an overview. Cancer Biother Radiopharm 2015;30:47–71.
5. Fani M, Maecke HR, Okarvi SM. Radiolabeled peptides: valuable tools for the detection and treatment of cancer. Theranostics 2012;2:481–501.
6. Lozza C, Navarro-Teulon I, Pelegrin A, Pouget JP, Vives E. Peptides in receptor-mediated radiotherapy: from design to the clinical application in cancers. Front Oncol 2013;3:247.
7. Bison SM, Konijnenberg MW, Melis M, Pool SE, Bernsen MR, Teunissen JJ, et al. Peptide receptor radionuclide therapy using radiolabeled somatostatin analogs: focus on future developments. Clin Transl Imaging 2014;2:55–66.
8. Stromblad S, Cheresh DA. Integrins, angiogenesis and vascular cell survival. Chem Biol 1996;3:881–5.
9. Jin H, Varner J. Integrins: roles in cancer development and as treatment targets. Br J Cancer 2004;90:561–5.
10. Desgrosellier JS, Cheresh DA. Integrins in cancer: biological implications and therapeutic opportunities. Nat Rev Cancer 2010;10:9–22.
11. Kaban K, Herbst RS. Angiogenesis as a target for cancer therapy. Hematol Oncol Clin North Am 2002;16:1125–71.
12. Lim EH, Danthi N, Bednarski M, Li KC. A review: integrin $\alpha_v\beta_3$-targeted molecular imaging and therapy in angiogenesis. Nanomedicine 2005;1:110–4.
13. Haubner R. Alphavbeta3-integrin imaging: a new approach to characterise angiogenesis? Eur J Nucl Med Mol Imaging 2006;33:S54–63.
14. Serini G, Valdembri D, Bussolino F. Integrins and angiogenesis: a sticky business. Exp Cell Res 2006;312:651–8.
15. Haubner R, Gratias R, Diefenbach B, Goodman SL, Jonczyk A, Kessler H. Structural and functional aspects of RGD-containing cyclic pentapeptides as highly potent and selective integrin $\alpha_v\beta_3$ antagonists. J Am Chem Soc 1996;118:7461–72.
16. Gaertner FC, Kessler H, Wester HJ, Schwaiger M, Beer AJ. Radiolabelled RGD peptides for imaging and therapy. Eur J Nucl Med Mol Imaging 2012;39:S126–38.
17. Liu Z, Wang F. Development of RGD-based radiotracers for tumor imaging and therapy: translating from bench to bedside. Curr Mol Med 2013;13:1487–505.
18. Janssen ML, Oyen WJ, Dijkgraaf I, Massuger LF, Frielink C, Edwards DS, et al. Tumor targeting with radiolabeled $\alpha_v\beta_3$ integrin binding peptides in a nude mouse model. Cancer Res 2002;62:6146–51.
19. Dijkgraaf I, Kruijtzer JA, Frielink C, Corstens FH, Oyen WJ, Liskamp RM, et al. $\alpha_v\beta_3$ Integrin-targeting of intraperitoneally growing tumors with a radiolabeled RGD peptide. Int J Cancer 2007;120:605–10.
20. Yoshimoto M, Ogawa K, Washiyama K, Shikano N, Mori H, Amano R, et al. $\alpha_v\beta_3$ Integrin-targeting radionuclide therapy and imaging with monomeric RGD peptide. Int J Cancer 2008;123:709–15.
21. Liu Z, Shi J, Jia B, Yu Z, Liu Y, Zhao H, et al. Two ^{90}Y-labeled multimeric RGD peptides RGD4 and 3PRGD2 for integrin targeted radionuclide therapy. Mol Pharm 2011;8:591–9.
22. Shi J, Fan D, Dong C, Liu H, Jia B, Zhao H, et al. Anti-tumor effect of integrin targeted ^{177}Lu-3PRGD$_2$ and combined therapy with Endostar. Theranostics 2014;4:256–66.
23. Bozon-Petitprin A, Bacot S, Gauchez AS, Ahmadi M, Bourre JC, Marti-Batlle D, et al. Targeted radionuclide therapy with RAFT-RGD radiolabelled with ^{90}Y or ^{177}Lu in a mouse model of $\alpha_v\beta_3$-expressing tumours. Eur J Nucl Med Mol Imaging 2015;42:252–63.
24. Galibert M, Jin ZH, Furukawa T, Fukumura T, Saga T, Fujibayashi Y, et al. RGD-cyclam conjugate: synthesis and potential application for positron emission tomography. Bioorg Med Chem Lett 2010;20:5422–5.
25. Jin ZH, Furukawa T, Galibert M, Boturyn D, Coll JL, Fukumura T, et al. Noninvasive visualization and quantification of tumor $\alpha_v\beta_3$ integrin expression using a novel positron emission tomography probe, ^{64}Cu-cyclam-RAFT-c(-RGDfK-)$_4$. Nucl Med Biol 2011;38:529–40.
26. Jin ZH, Razkin J, Josserand V, Boturyn D, Grichine A, Texier I, et al. *In vivo* noninvasive optical imaging of receptor-mediated RGD internalization using self-quenched Cy5-labeled RAFT-c(-RGDfK-)$_4$. Mol Imaging 2007;6:43–55.
27. Sancey L, Garanger E, Foillard S, Schoehn G, Hurbin A, Albiges-Rizo C, et al. Clustering and internalization of integrin $\alpha_v\beta_3$ with a tetrameric RGD-synthetic peptide. Mol Ther 2009;17:837–43.
28. Smith SV. Molecular imaging with copper-64. J Inorg Biochem 2004;98:1874–901.

29. Connett JM, Anderson CJ, Guo LW, Schwarz SW, Zinn KR, Rogers BE, et al. Radioimmunotherapy with a ^{64}Cu-labeled monoclonal antibody: a comparison with ^{67}Cu. Proc Natl Acad Sci U S A 1996;93:6814–8.
30. Anderson CJ, Jones LA, Bass LA, Sherman EL, McCarthy DW, Cutler PD, et al. Radiotherapy, toxicity and dosimetry of copper-64-TETA-octreotide in tumor-bearing rats. J Nucl Med 1998;39:1944–51.
31. Lewis JS, Lewis MR, Cutler PD, Srinivasan A, Schmidt MA, Schwarz SW, et al. Radiotherapy and dosimetry of ^{64}Cu-TETA-Tyr^3-octreotate in a somatostatin receptor-positive, tumor-bearing rat model. Clin Cancer Res 1999;5:3608–16.
32. Lewis J, Laforest R, Buettner T, Song S, Fujibayashi Y, Connett J, et al. Copper-64-diacetyl-bis(N4-methylthiosemicarbazone): An agent for radiotherapy. Proc Natl Acad Sci U S A 2001;98:1206–11.
33. Jin ZH, Furukawa T, Sogawa C, Claron M, Aung W, Tsuji AB, et al. PET imaging and biodistribution analysis of the effects of succinylated gelatin combined with L-lysine on renal uptake and retention of ^{64}Cu-cyclam-RAFT-c(-RGDfK-)$_4$ *in vivo*. Eur J Pharm Biopharm 2014;86:478–86.
34. Jin ZH, Furukawa T, Claron M, Boturyn D, Coll JL, Fukumura T, et al. Positron emission tomography imaging of tumor angiogenesis and monitoring of antiangiogenic efficacy using the novel tetrameric peptide probe ^{64}Cu-cyclam-RAFT-c(-RGDfK-)$_4$. Angiogenesis 2012;15:569–80.
35. Rolleman EJ, Melis M, Valkema R, Boerman OC, Krenning EP, de Jong M. Kidney protection during peptide receptor radionuclide therapy with somatostatin analogues. Eur J Nucl Med Mol Imaging 2010;37:1018–31.
36. Eckerman EF, Endo A. MIRD: Radionuclide Data and Decay Schemes (2nd Edition). Reston: Soc Nucl Med 2010 p. 103.
37. Yoshida C, Tsuji AB, Sudo H, Sugyo A, Kikuchi T, Koizumi M, et al. Therapeutic efficacy of c-kit-targeted radioimmunotherapy using 90Y-labeled anti–c-kit antibodies in a mouse model of small cell lung cancer. PLoS ONE 2013;8:e59248.
38. Buchsbaum DJ, Langmuir VK, Wessels BW. Experimental radioimmunotherapy. Med Phys 1993;20:551–67.
39. Veeravagu A, Liu Z, Niu G, Chen K, Jia B, Cai W, et al. Integrin $\alpha_v\beta_3$-targeted radioimmunotherapy of glioblastoma multiforme. Clin Cancer Res 2008;14:7330–9.
40. Hintzen RQ, Voormolen J, Sonneveld P, van Duinen SG. Glioblastoma causing granulocytosis by secretion of granulocyte-colony-stimulating factor. Neurology 2000;54:259–61.
41. Ahn HJ, Park YH, Chang YH, Park SH, Kim MS, Ryoo BY, et al. A case of uterine cervical cancer presenting with granulocytosis. Korean J Intern Med 2005;20:247–50.
42. Janssen M, Frielink C, Dijkgraaf I, Oyen W, Edwards DS, Liu S, et al. Improved tumor targeting of radiolabeled RGD peptides using rapid dose fractionation. Cancer Biother Radiopharm 2004;19:399–404.
43. Lewis JS, Wang M, Laforest R, Wang F, Erion JL, Bugaj JE, et al. Toxicity and dosimetry of ^{177}Lu-DOTA-Y3-octreotate in a rat model. Int J Cancer 2001;94:873–7.
44. Cremonesi M, Ferrari M, Bodei L, Tosi G, Paganelli G. Dosimetry in Peptide radionuclide receptor therapy: a review. J Nucl Med 2006;47:1467–75.
45. Novak-Hofer I, Schubiger PA. Copper-67 as a therapeutic nuclide for radioimmunotherapy. Eur J Nucl Med Mol Imaging 2002;29:821–30.